

PROXIMAL FEMUR 3-D MORPHOLOGICAL ANALYSIS UTILIZING STATISICAL BONE ATLAS

M. R. Mahfouz, E. E. Abdel Fatah, H. EL Dakhakhni, R. T. Mesiha, K. R. Kesler, L. N. Smith

Center for Musculoskeletal Research, University of Tennessee, Knoxville, TN, USA

e-mail: mmahfouz@utk.edu

Abstract- The study of proximal femur shape and bone quality play major roles in design of orthopedic implants, mainly for the hip. Moreover the quantification of anatomical difference between male and female is always an active and important area in forensic science. Most measurements and previous designs were based on assessment of bone using 2D X-Ray. Several errors might rise in ordinary 2D X-Ray due to internal or external rotation of the femur relative to the plane of imaging, magnification factor, and the X-Ray technique used for imaging, which might wash out some of the important landmarks that can affect the results. In this paper we present a new method for evaluation of proximal femur shape and Bone Quality based on three dimensional measurements utilizing statistical bone atlas. Comparison between our results and previous published results is presented.

Keywords - proximal femur, intramedullary canal, morphology, statistical bone atlas, intramedullary (IM) canal

I. INTRODUCTION

X-rays radiographs still play a fundamental role in the preoperative planning of total hip arthroplasty (THA) [3], which requires standardized radiographic views of the hip. To provide proper orientation on the anteroposterior (AP) projection, the proximal femur must be positioned so that the long axis of the femoral neck should be perpendicular to the radiographic cassette and perpendicular to the X-ray beam. Similarly for the lateral projection, the long axis of the femoral neck should be perpendicular to cassette and parallel to the X-ray beam. To obtain this projection the femur must be internally rotated to compensate for the normal anteversion of the head and neck.

Occasionally, the femur head is externally rotated, either because the X-rays procedure did not properly compensate for femoral torsion or many patients suffering from hip joint arthritis are unable to internally rotate the femur. Moreover, most X-rays templates have been designed on the assumption that the widest mediolateral (ML) dimension of the proximal canal is visualized on this AP projection, and that the prosthesis will ultimately fit in the canal in this orientation. These assumptions may not be correct for a number of reasons. First, the widest dimension of the canal is often not visible on the true AP X-ray as in the cases of osteopenia. Second, the overall shape of intramedullary (IM) canal may vary with age, sex, disease and other complex factors. Different studies were previously presented that study the shape of IM canal and its change with aging and how this can affect the design of hip implants, however most of these studies were using 2-D plane X-Ray radiographs [4-9].

The objectives of this study are to provide 3-D measurements in order to investigate the relationship between the bone quality and the IM canal shape. In addition to determination of both the effect of femoral rotation on the X-rays dimensions of the femur (especially proximal femur where prosthetic sizing of THA is

more important) and the variation of femoral rotation that can affect the accuracy of femoral tem plating.

II. MATERIALS AND METHODS

In order to eliminate subjectivity in our analysis a set of landmarks with anatomical and surgical significance were automatically detected on both femur and IM canal; these landmarks were accurately detected using the power of statistical bone atlases. These landmarks were used to automate different 3-D measurements on both femur and IM canal. A total of 146 cases divided into 61 females and 85 males were used in this study.

A. Atlas Creation

CT datasets of both femur and corresponding IM canal were manually segmented. Segmented femur models were added to the atlas. Adding a new model to the atlas involves different steps starting from rigid alignment (iterative closest point ICP) of base and the new model, affine warping, and non-linear warping of the base mesh (mutual correspondence warping). More information on atlas creation and use can be found in [1, 2]. For every atlas femur the corresponding IM Canal was registered to the same coordinate space using ICP. In order to evaluate the accuracy of IM canal segmentation an automatic segmentation method was developed. Below is a description of the segmentation algorithm.

Dicom slices are binarized using Otsu thresholding, and then the canal boundary is traced. The lesser trochantric slices are defined as having an elliptic cross section rather than the circular cross section seen along the rest of the IM canal. The start of the lesser trochanter is identified by the ratio between the two principal components of the contour (performed by PCA). The calcar septum is automatically removed from the lesser trochantric slices. The intensity levels of the calcar septum vary throughout the slices of the lesser trochanter. For slices where the calcar septum has high intensity, the calcar septum tip is extracted by calculating the K-mean curvature (with $k = 8$) where the tip is defined as the point having maximum curvature (point 1 in Fig. 1a). The corresponding medial/lateral point along the contour which lies posterior to the tip is then located (point 2 in Fig. 1a). The calcar septum is then removed from the contour, seen in Fig. 1b. For slices with weak contrast of the calcar septum or slices with no distinguishable calcar septum (e.g. start of the lesser tochanter), the two cut points (Fig. 1a) are estimated using the nearest slice with the points defined.

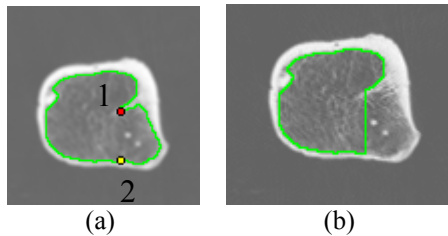


Fig. 1. Automatic segmentation of calcar area. a) calcar septum tip (point 1) and corresponding posterior point along contour (point 2) b) contour after removal of calcar septum.

B. Landmarks and Axes Calculation

An important landmark that is usually used as the main reference in most proximal femur analyses is the midpoint of the lesser trochanter. This point is defined as the most protruding point in the middle of the lesser trochanter. Two other landmarks that have significant importance are the femur and IM Canal isthmi. In order to calculate these two landmarks, a region of interest is defined on the femur and IM canal between 10% and 90% of the total femur length. Both models are then intersected with planes normal to the anatomical axis at 0.5mm intervals (see Fig. 2). One method for finding the isthmus includes calculating area and circumference for each of these contours. The isthmus is then defined as the contour having the smallest area. Another method for determining the isthmus, and the one used here, is to least square fit a circle to the femur and IM contours and find the circle with minimum diameter, shown in Figs. 2 and 3.

C. 3-D Measurements:

Using the bone atlas and automatically calculated landmarks and axes, different measurements were made that describe the shape of the IM canal and at the same time give indication about change in the bone quality. Highlighted below are some of these measurements:

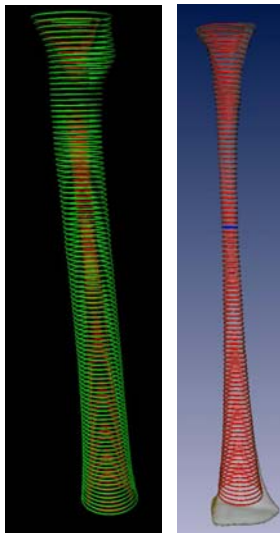


Fig. 2. Femur shaft circle in green and IM Canal in red, IM Canal isthmus in blue.

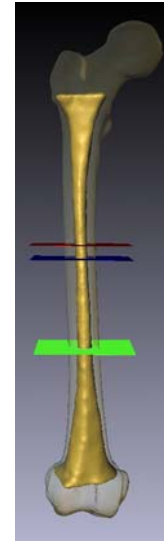


Fig. 3. IM isthmus Plane in blue, femur isthmus plane in green, 10 cm reference plane in red.

IM canal radius to femur radius ratio: the ratio between radius of the IM canal fitted circle to the radius of femur fitted circle as shown in Fig. 4. Measured at femur isthmus level it is designated 'RRFW', at IM canal isthmus level it is designated 'RRIW', and average ratio along femur shaft is designated 'ARR'. IM canal area to femur area ratio: at femur isthmus it is designated 'ARFW', at IM Canal isthmus it is 'ARIW', and average ratio along femur shaft is designated 'AAR'. Difference between Femur radius and IM radius: at femur isthmus level is designated 'RDFW' and at IM isthmus level is designated 'RDIW'.

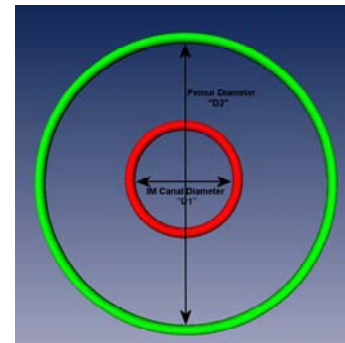


Fig. 4. IM radius to femur radius ratio.

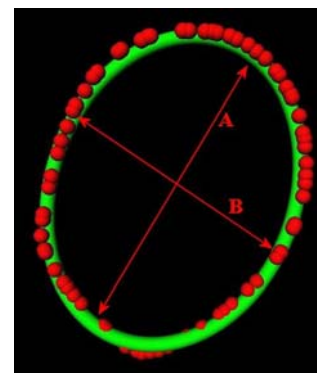


Fig. 5. B/A ratio at IM Isthmus.

ABR ratio: measurement that helps identifying the direction of the bone loss. It is defined as the ratio between the minor axis 'B' and major axis 'A' of the fitted ellipse to the IM canal contour at the level of the narrowest point on IM Canal as shown in Fig. 5.

CIA: defined by (1) where Z is the femur area at 10 cm below mid lesser trochanter point and X is the IM canal area at the same level.

$$\frac{(Z - X)}{Z} \quad (1)$$

CCA: ratio between IM canal area at 3 cm below mid-lesser trochanter level to the IM canal area at level of 10 cm below mid-lesser trochanter. These measurements are equivalent to the 2-D measurement Cortical Index 'CI' and canal to calcar isthmus ratio 'CC' conducted by Dorr et al. [9].

XYRA: ratio between IM canal area at 3 cm below mid-lesser trochanter level to the canal area at level of 10 cm below mid-lesser trochanter.

D. Effect of Rotation on 2-D X-Ray Measurements

As a way to measure the reliability of the 3-D measurements, we studied the effect of rotation of the femur relative to the image plane on automatic 2-D measurements conducted on X-Ray. We used digitally reconstructed radiographs (DRRs), which are synthetic X-rays generated by casting rays according to specific camera geometry through a CT volume [10].

Ten cases were used to conduct this experiment where each case was placed in three different positions relative to the imaging plane, first with posterior condylar axis 'PCA' aligned to the plane as the plane of imaging: this was considered as the normal anatomical position. The model was then internally rotated 10 degrees followed by a 12 degrees external rotation.

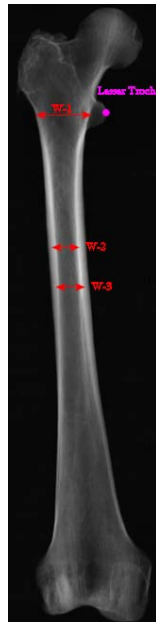


Fig. 6. 2-D measurements conducted on the DRRs.

Fig. 6 shows the DRR 2-D measurements where W-1 is the IM canal width on the same level of lesser trochanter, W-2 is the IM canal width at 10 cm below lesser trochanter and W-3 is the IM canal width at the IM canal isthmus.

III. RESULTS

Table I highlights the mean, standard deviation, T-test score and power test results for each of the 3-D measurements for both males and females. Table II shows the percentage error in 2-D measurements with the 10° internal rotation, where Table III shows the percentage error with the 12° external rotation. Fig. 7 shows comparison between manual and automatic segmentation of IM canal.

IV. DISCUSSION

The 3-D measurements results were all statistically significant between males and females with all $p < 0.01$. It was noticed that females in general have higher RRFW, RRIW, ARFW, ARIW, AAR, and ARR which in turns reflect the fact that females suffer more from bone loss especially after the end of menopause. Fig. 8 shows effect of the change in the RRFW on the shape of the IM

TABLE I
3-D MEASUREMENTS RESULTS FOR MALE AND FEMALE

| | Female | | Test | | Male | |
|------|--------|----------|-------|-------|-------|----------|
| | μ | σ | T | Power | μ | σ |
| CIA | 0.76 | 0.09 | <0.01 | 71 | 0.80 | 0.06 |
| CCA | 0.57 | 0.12 | <0.01 | 136 | 0.52 | 0.09 |
| XYRA | 0.29 | 0.10 | <0.02 | 155 | 0.25 | 0.06 |
| ABR | 0.72 | 0.08 | <0.01 | 46 | 0.78 | 0.06 |
| RRFW | 0.51 | 0.09 | <0.01 | 57 | 0.46 | 0.06 |
| RRIW | 0.48 | 0.09 | <0.01 | 50 | 0.42 | 0.06 |
| ARFW | 0.26 | 0.09 | <0.01 | 58 | 0.22 | 0.06 |
| ARIW | 0.23 | 0.09 | <0.01 | 53 | 0.18 | 0.05 |
| ARR | 0.62 | 0.06 | <0.01 | 51 | 0.58 | 0.05 |
| AAR | 0.39 | 0.07 | <0.01 | 58 | 0.35 | 0.05 |
| RDFW | 0.64 | 0.12 | <0.01 | 16 | 0.78 | 0.10 |
| FDIW | 0.70 | 0.13 | <0.01 | 15 | 0.85 | 0.09 |

TABLE II
PERCENTAGE ERROR IN 2-D MEASUREMENTS DUE TO 10° INTERNAL ROTATION

| | W-1 | W-2 | W-3 |
|----------|-------|-------|-------|
| μ | 5.84% | 3.83% | 1.41% |
| σ | 6.23% | 1.73% | 1.75% |

TABLE III
PERCENTAGE ERROR IN 2-D MEASUREMENTS DUE TO 12° EXTERNAL ROTATION

| | W-1 | W-2 | W-3 |
|----------|-------|-------|-------|
| μ | 7.90% | 4.62% | 2.25% |
| σ | 5.90% | 3.01% | 2.51% |

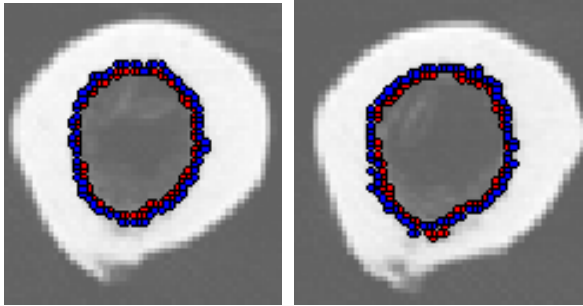


Fig. 7. Automatic segmentation in red and manual in blue.

canal and the quality of the bone; it can be notice how the case with higher ratio suffers more from bone loss.

By looking at the CCA and XYRA, females are noticed to have higher ratio which implies that females have a more stove pipe shaped IM canal. Another interesting finding was the ABR ratio where it was noticed that females have a lower ratio which means that they have a more elliptical shaped IM canal. Effect of bone rotation on 2-D measurements from X-Ray showed a percentage error with rotation. This in turn highlights how accurate 3-D measurements are compared to ordinary 2-D X-Ray measurements.

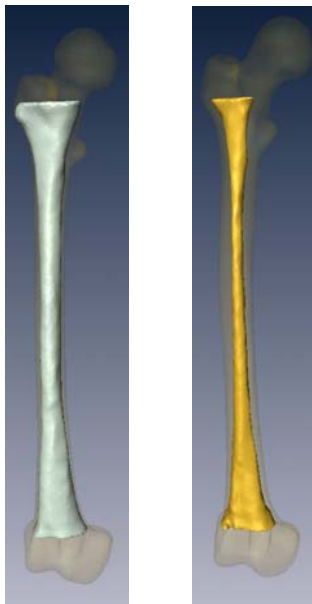


Fig. 8. Two models showing the effect of the change in the radii ratio. Silver model radii ratio of 0.69 and golden model with radii ratio of 0.38.

V. CONCLUSION

In this paper we proposed automated 3-D measurements on both IM canal and proximal femur. These measurements were found statistically significant between males and females which reflect the difference in anatomy. Moreover these measurements are an indication of the changes in IM canal shape and bone quality due to aging, osteoporosis and osteopenia. Unlike some of the previous work, our method is fully automated, accurate and repeatable which provides more accurate results over manual techniques. We presented a study to show the effect of rotation of the bone relative to the image plane on the 2-D measurements

performed on X-Ray. The error generated as effect of the rotation provides more support for why 3-D measurements are more reliable and accurate.

REFERENCES

- [1] Mahfouz, M.R., Booth, R.E., Jr, Argenson, J.N, Merkl, B.C., Abdel Fatah, E.E., Kuhn, M.J., "Analysis of Variation of Adult Femora Using Sex-Specific Statistical Atlases", 7th Intl Symp CMBBE, Antibes, Cote d'Azur, France, 2006.
- [2] Mahfouz, M.R., Badawi, A.M., Merkl, B.C., Abdel Fatah, E.E., Pritchard, E.R., Kesler, K., Moore, M., Jantz, R., "3D Statistical Shape Models of Patella for Sex Classification", 28th Annual IEEE EMBS, New York, 2006.
- [3] Gruen, T. A., 1997, "A Simple Assessment of Bone Quality Prior to Hip Arthroplasty: Cortical Index Revisited," *Acta Orthop. Belg.*, 63 Suppl 1, pp. 20–27.
- [4] Yeung, K. Chiu, W. Yau, W. Tang, W. Cheung, T. Ng, "Assessment of the Proximal Femoral Morphology Using Plain Radiograph—Can it Predict the Bone Quality?", *J Arthroplasty*. 2006 Jun;21(4):508-13.
- [5] Koot VC, Kesselaer SM, Clevers GJ, de Hooge P, Weits T, van der Werken C, "Evaluation of the Singh index for measuring Osteoporosis", *J Bone Jt Surg Br* 1996;78:831.
- [6] Noble, P. C., Box, G. G., Kamaric, E., Fink, M. J., Alexander, J. W., and Tullow, H. S., 1995, "The Effect Of Aging On The Shape Of The Proximal Femur", *Clin. Orthop. Relat. Res.*, 316, pp. 31–44.
- [7] Noble PC, Alexander JW, Lindahl LJ, Yew DT, Granberry WM, Tullos HS, "The anatomic basis of femoral component design", *Clin Orthop*.1988; 235:148 -65.
- [8] Eckrich SG, Noble PC, Tullos HS, "Effect of rotation on the radiographic appearance of the femoral canal", *J Arthroplasty*. 1994 Aug;9(4):419-26.
- [9] Dorr LD, Faugere MC, Mackel AM, Gruen TA, Bognar B, Malluche HH., "Structural and cellular assessment of bone quality of the proximal femur", *Bone*.1993; 14:231 -42
- [10] Russakoff D., Rohlfing T., Rueckert D., Shahidi R., Kim D. and Maurer C., "Fast calculation of digitally reconstructed radiographs using light fields", *Proc. SPIE*, 2003, Vol. 5032, 684-695.